Supporting Information

Covalent Organic Frameworks for Simultaneous CO_2 Capture and Selective Catalytic Transformation

Yaling Li,[†] Jianqiang Zhang,[†] Kaiming Zuo,[†] Zhongping Li,[‡] Yu Wang,[§] Hui Hu,[†] Chaoyuan Zeng,*[,†] Huanjun Xu,[†] Baoshan Wang,*[, #] and Yanan Gao*[,†]

[†] Key Laboratory of Ministry of Education for Advanced Materials in Tropical Island Resources, Hainan University, No 58, Renmin Avenue, Haikou 570228, P. R. China;

[‡] Department of Chemistry, Faculty of Science, National University of Singapore, 3 Science Drive 3, 117543, Singapore;

[§] School of Light Industry and Chemical Engineering, Dalian Polytechnic University, 1 Qinggongyuan, Dalian 116034, P. R. China;

[#] Key Laboratory of Biomedical Polymers (Ministry of Education), College of Chemistry and Molecular Sciences, Wuhan University, Wuhan 430072, P. R. China.

Table S1. Elemental analysis of Co(II)@TA-TF COF.

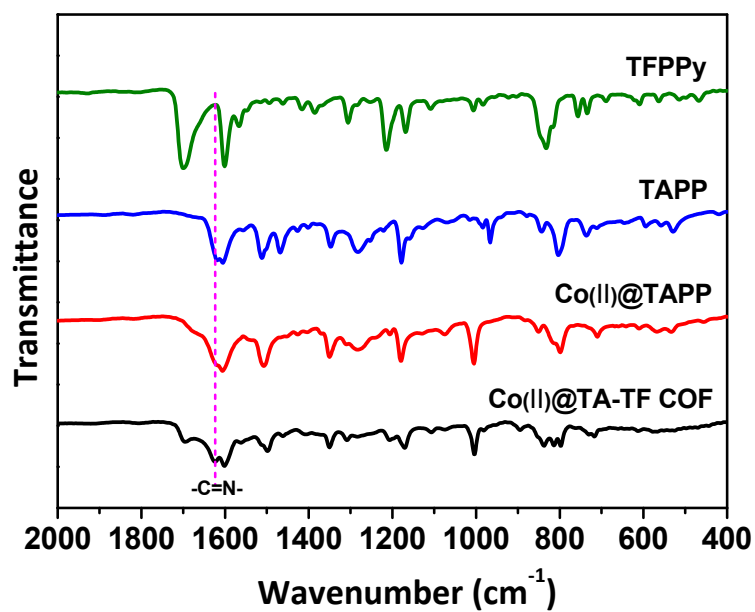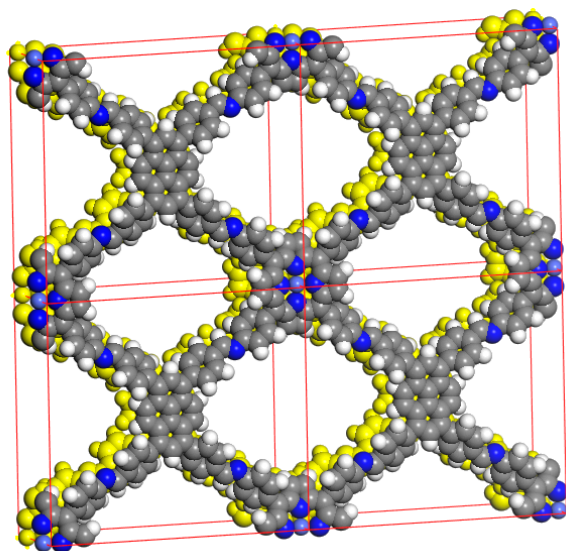| Sample	Molecular formula	Elemental analysis (Calcd.)			Elemental analysis (Found)		
		N [wt%]	C [wt%]	H [wt%]	N [wt%]	C [wt%]	H [wt%]
Co(II)@TA-TF COF	$(C_{88}H_{54}N_8Co)_n$	8.74%	82.42%	4.24%	8.14%	80.90%	4.01%

Figure S1. FTIR spectra of Co(Ⅱ)@TA-TF COF, Co(Ⅱ)@TAPP, TAPP and TFPPy.

Firstly, the TA-TA + TF-TF AA stacking model (space group: Pmmm) was constructed and optimized. Apparently, the shoulder peak at 5.4 is absent (Figure S2).
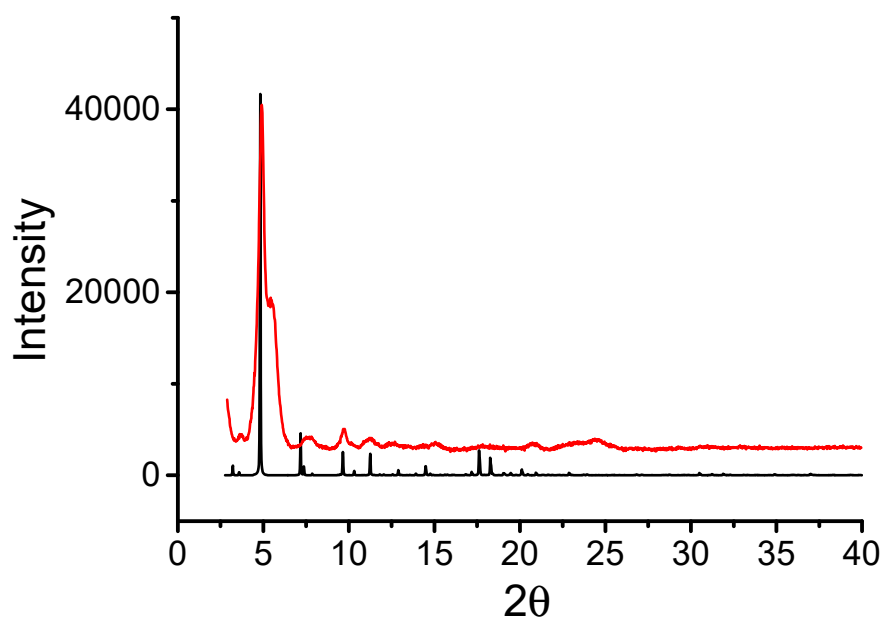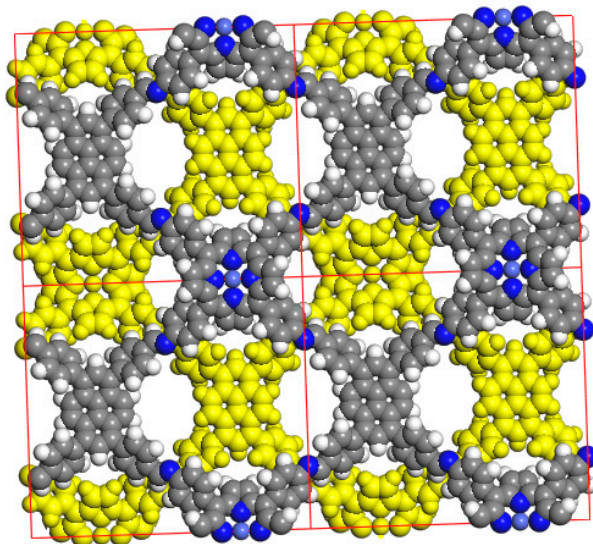
Figure S2. Comparison of experimentally observed PXRD pattern and calculated profile based on the true TA-TA + TF-TF AA eclipsed packing structure.

The staggered AB-stacking structure (space group: Pmma) is more stable than the true AA stacking structure by 17 kcal/mol, however, the XRD plot does not match the experimental one yet (Figure S3).
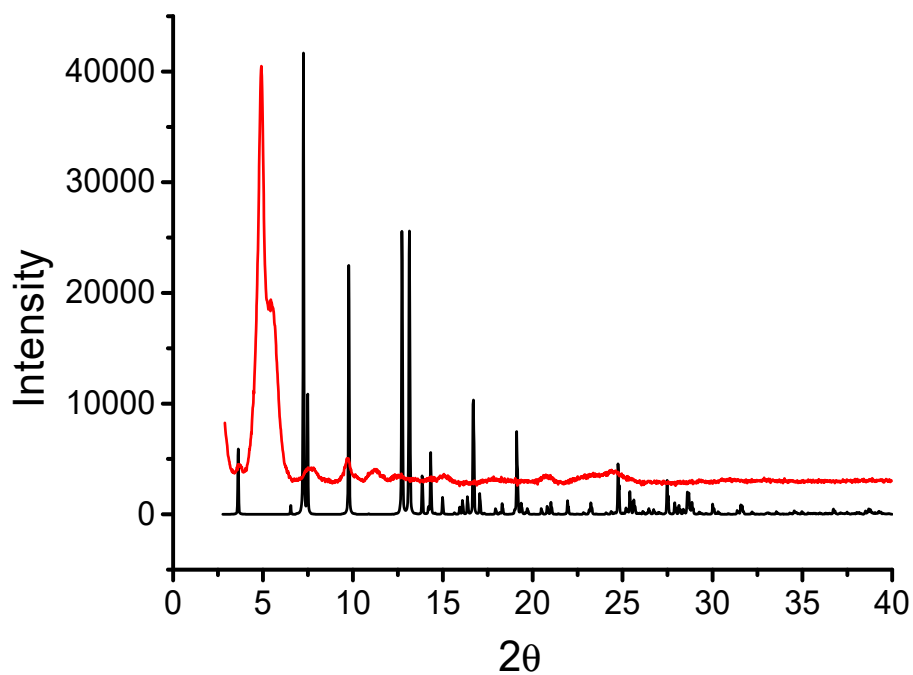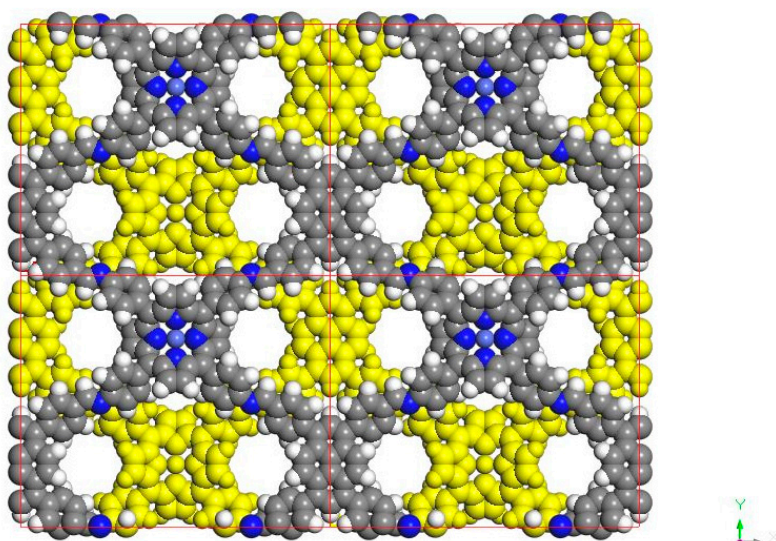
Figure S3. Comparison of experimentally observed PXRD pattern and calculated profile based on the one staggered AB-stacking structure.

An alternative staggered AB-stacking structure (space group: Pmma), as shown in Figure S4, was also constructed and optimized. However, the energy of this structure is 5 kcal/mol higher than that of the structure listed in Figure S3. Moreover, the PXRD plot does not match the experimental one yet.

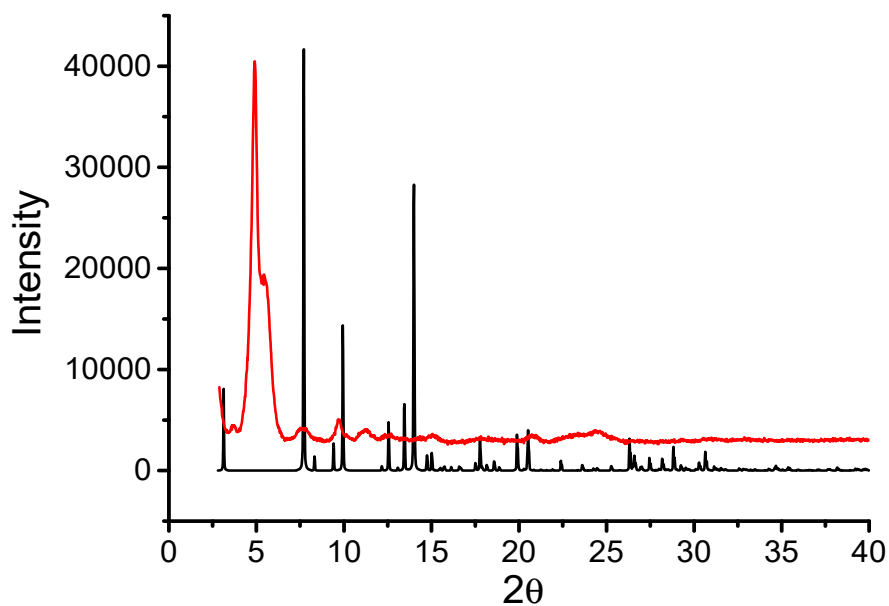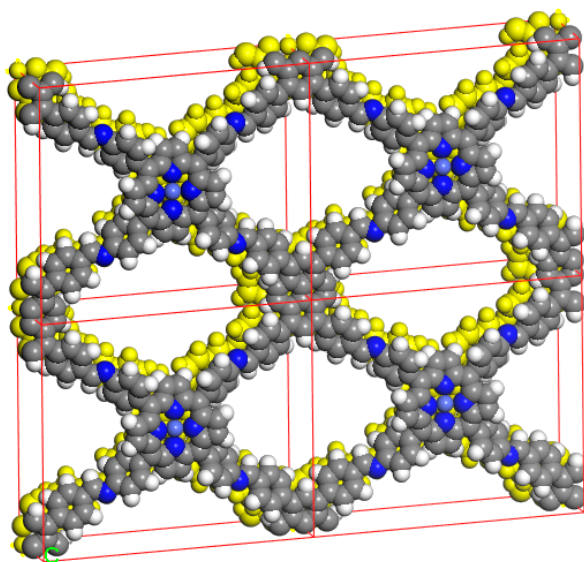**Figure S4**. Comparison of experimentally observed PXRD pattern and calculated profile based on the alternative staggered AB-stacking structure.

Then, the TA-TF AA stacking model (space group: Pmmn) was constructed and optimized. This structure is more stable than the TA-TA + TF-TF stacking model, as indicated by the fact that its energy is 48 kcal/mol lower (Figure S5). However, the shoulder peak is still missing.

Figure S5. Comparison of experimentally observed PXRD pattern and calculated profile based on the true TA-TF AA stacking model.

In this case, the slipped TA-TF AA structure was considered by optimizing the slipping distance Δd. The minimum (space group: P-1) was located at Δd = *1.7* Å (along *xy* direction), the energy is lowered by 6 kcal/mol. In this case, the theoretical XRD pattern matches the experimental graph very well (Figure S6). Refinement results in *Rwp* = 5.75%, and *Rp* = 3.51%.
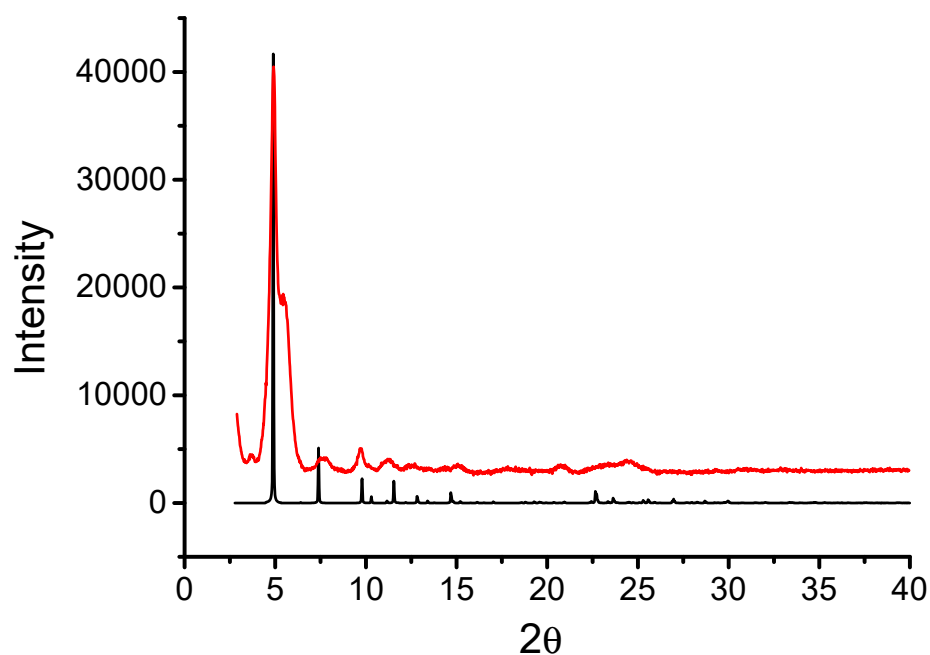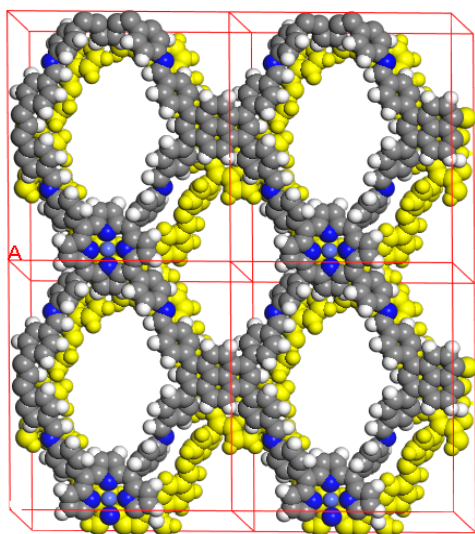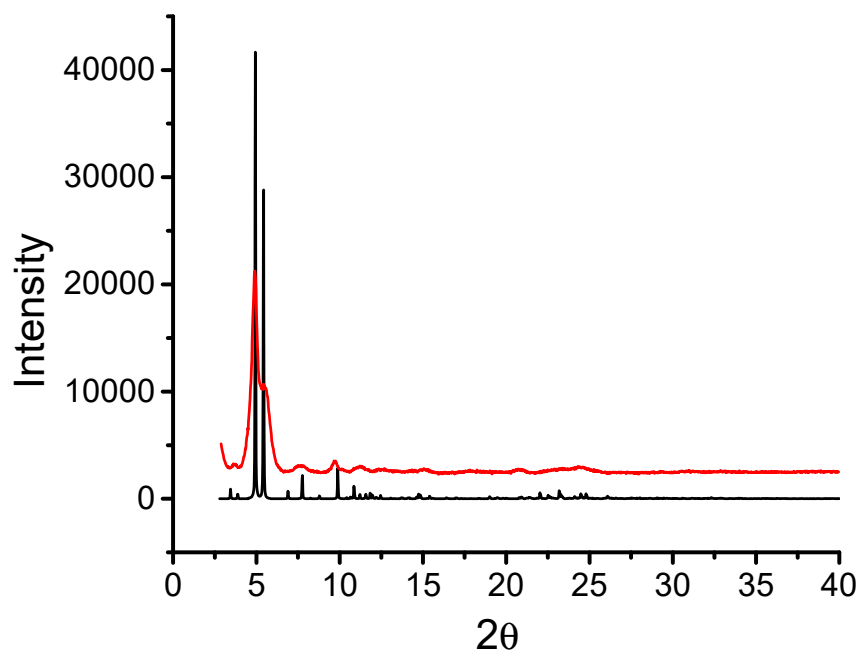
Figure S6. Comparison of experimentally observed PXRD pattern and calculated profile based on the slipped TA-TF AA structure with a slight interlayer horizontal offset of 1.7 Å. This structure was described in the text, as shown by Figure 1.

Table S2. Fractional atomic coordinates for unit cell of Co(II)@TA-TF COF calculated using the density-functional tight-binding method after performing the Pawley refinement.

Slipped TA-TF AA structure	Space group: Triclinic P-1 a = 8.5899 Å, b = 23.0876 Å, c = 25.8289 Å α = 83.7391°, β = 95.0091°, γ = 97.6533°		
C	-1.07899	-0.55505	-0.31829
H	-1.13532	-0.53139	-0.29181
C	-0.99213	-0.52199	-0.35664
H	-0.98087	-0.47371	-0.35899
C	-1.06010	-1.13055	-0.88848
H	-1.16434	-1.16182	-0.89797
C	-0.99337	-1.09342	-0.92898
H	-1.04834	-1.09578	-0.96892
C	-0.24875	-0.63848	-1.08671
H	-0.24084	-0.68592	-1.07941
C	-0.23116	-0.60502	-1.04429
H	-0.21385	-0.62658	-1.00441
C	-1.07726	-1.12062	-0.54617
H	-0.96327	-1.13438	-0.55275
C	-1.08502	-1.08309	-0.50774
H	-0.97747	-1.06748	-0.48434

N	-0.81340	-0.53389	-0.47792
C	-1.36521	-0.79365	-0.32275
H	-1.37893	-0.81428	-0.35960
C	-1.41195	-0.82746	-0.27531
C	-1.44932	-0.88973	-0.27094
C	-1.09856	-0.61718	-0.31386
C	-0.92557	-0.54958	-0.39396
C	-0.84370	-0.51329	-0.43593
H	-0.80902	-0.46580	-0.42909
C	-1.10811	-1.09888	-0.73532
H	-1.07005	-1.05860	-0.75979
C	-1.12237	-1.15790	-0.74985
C	-1.06522	-1.17294	-0.79510
C	-1.07047	-1.23234	-0.80283
C	-1.00013	-1.25181	-0.84543
H	-0.91842	-1.22501	-0.87134
C	-0.99774	-1.12847	-0.83618
C	-0.85947	-1.05254	-0.91851
C	-0.71323	-0.97043	-1.14244
H	-0.76108	-0.98029	-1.18185
C	-0.77195	-1.00603	-1.09975
H	-0.86404	-1.04304	-1.10637
H	-0.69337	-0.35486	-0.57361
C	-0.75786	-0.43673	-0.52802
H	-0.84242	-0.41754	-0.50744
C	-1.28029	-0.91892	-0.33727
H	-1.18537	-0.88430	-0.32686
C	-1.25657	-0.95549	-0.37464
H	-1.14459	-0.94916	-0.39339
C	-0.16101	-0.47163	-0.83101
H	-0.09560	-0.48166	-0.79319
C	-0.15687	-0.50707	-0.87127
H	-0.08592	-0.54389	-0.86539
N	-0.78518	-1.01515	-0.95820
C	-0.47269	-0.73044	-1.14813
H	-0.50419	-0.70501	-1.11781
C	-0.37300	-0.70232	-1.18780
C	-0.28539	-0.64572	-1.18469
C	-0.59696	-0.92193	-1.13571
C	-0.71979	-0.99376	-1.04830
C	-0.78890	-1.03148	-1.00456
H	-0.84725	-1.07595	-1.01440
C	-0.51468	-0.44648	-0.70384
H	-0.60086	-0.48091	-0.68682
C	-0.44991	-0.39298	-0.68181

C	-0.46704	-0.38239	-0.63033
C	-0.38204	-0.33232	-0.61047
C	-0.36762	-0.32304	-0.55592
H	-0.40760	-0.35490	-0.52375
C	-0.56575	-0.42364	-0.59429
C	-0.73700	-0.49669	-0.51725
C	-0.46304	-1.02612	-0.67544
H	-0.35204	-1.01814	-0.69480
C	-0.48599	-0.98995	-0.63778
H	-0.39256	-0.95447	-0.62797
C	0.33299	-0.58779	-1.11329
H	0.40292	-0.62487	-1.10711
C	0.33003	-0.55263	-1.07292
H	0.40139	-0.56140	-1.03607
C	-0.46021	-1.08861	-0.91585
H	-0.55808	-1.12348	-0.92282
C	-0.39794	-1.05408	-0.95874
H	-0.44350	-1.06347	-0.99852
C	-0.44909	-0.51590	-0.41511
H	-0.53352	-0.49679	-0.39439
C	-0.36349	-0.47980	-0.45238
H	-0.38147	-0.43327	-0.46025
N	-0.76220	-0.96948	-0.54241
C	0.30426	-0.26427	-0.67661
H	0.27520	-0.28870	-0.63902
C	0.28420	-0.29374	-0.72347
C	0.19494	-0.35011	-0.72730
C	-0.57796	-1.07312	-0.68804
C	-0.62618	-0.99875	-0.61171
C	-0.64488	-0.96055	-0.57146
H	-0.54914	-0.92263	-0.56737
C	0.44385	-0.55068	-1.25112
H	0.46013	-0.51580	-1.22490
C	0.34104	-0.60485	-1.24401
C	0.24496	-0.61846	-1.20236
C	0.15484	-0.67332	-1.19557
C	0.05550	-0.69007	-1.15307
H	0.02913	-0.66105	-1.12508
C	0.24665	-0.57694	-1.16152
C	0.23759	-0.50573	-1.07972
C	0.27051	-0.44954	-0.85429
H	0.28626	-0.47189	-0.81470
C	0.25153	-0.48306	-0.89655
H	0.25271	-0.53093	-0.88949
C	-0.64151	-0.87671	-0.43292
H	-0.53379	-0.86137	-0.40951

|			
C	-0.63210	-0.91342	-0.47162
H	-0.51768	-0.92738	-0.47731
C	0.02246	-0.35547	-0.65073
H	0.02715	-0.30731	-0.65380
C	-0.05780	-0.38856	-0.61056
H	-0.10903	-0.36613	-0.58197
C	-0.13115	-0.91425	-1.17426
H	-0.18249	-0.91717	-1.21457
C	-0.19831	-0.95199	-1.13393
H	-0.30150	-0.98396	-1.14285
N	0.23281	-0.46973	-1.03952
C	-0.46761	-1.21149	-0.85273
H	-0.39191	-1.19181	-0.88388
C	-0.50212	-1.17625	-0.81362
C	-0.46465	-1.11391	-0.81744
C	0.27174	-0.38796	-0.86167
C	0.23341	-0.45631	-0.94812
C	0.22198	-0.49247	-0.99191
H	0.20632	-0.54137	-0.98135
C	-0.85550	-0.89942	-0.31526
H	-0.86112	-0.93535	-0.34003
C	-0.81454	-0.83821	-0.33159
C	-0.78717	-0.81694	-0.38313
C	-0.74284	-0.75702	-0.39608
C	-0.85550	-0.89942	-0.31526
H	-0.86112	-0.93535	-0.34003
C	-0.81454	-0.83821	-0.33159
C	-0.78717	-0.81694	-0.38313
C	-0.74284	-0.75702	-0.39608
C	-0.71078	-0.73219	-0.44813
H	-0.74070	-0.75427	-0.48377
C	-0.78608	-0.85853	-0.42382
C	-0.76874	-0.93298	-0.50262
N	-0.15957	-0.27933	-0.77561
N	-0.30574	-0.28416	-0.63970
Co	-0.25094	-0.27866	-0.71060
N	-1.17742	-1.19588	-0.70927
N	-0.34794	-0.35857	-0.71561
C	-1.50772	-0.91831	-0.22445
C	-1.42749	-0.79605	-0.23154
H	-1.11902	-0.58212	-0.22140
C	-1.19577	-0.62351	-0.22614
C	-1.36289	-0.73518	-0.23222
H	-1.52742	-0.96665	-0.22023
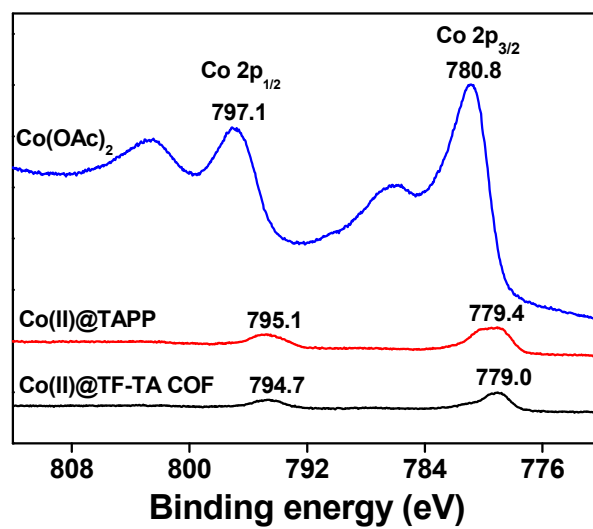
Figure S7. XPS results (Co 2p) for Co(OAc)₂, Co(II)@TAPP and Co(II)@TA-TF COF.
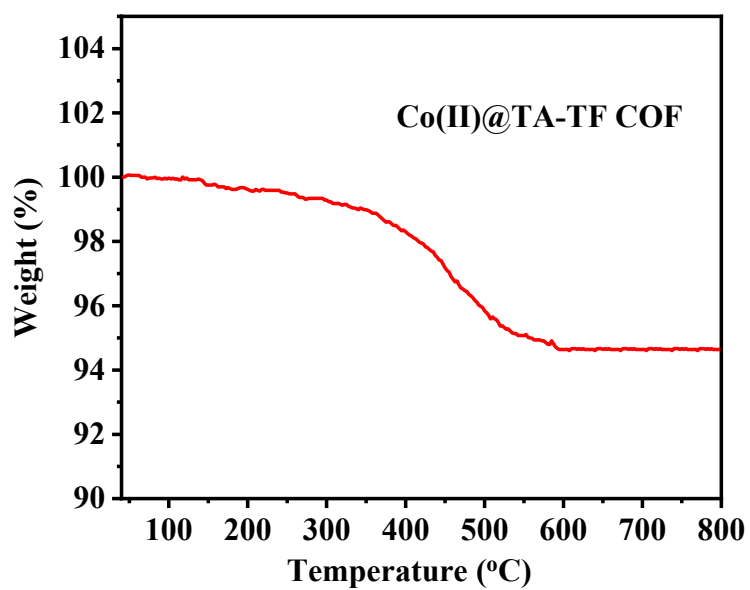

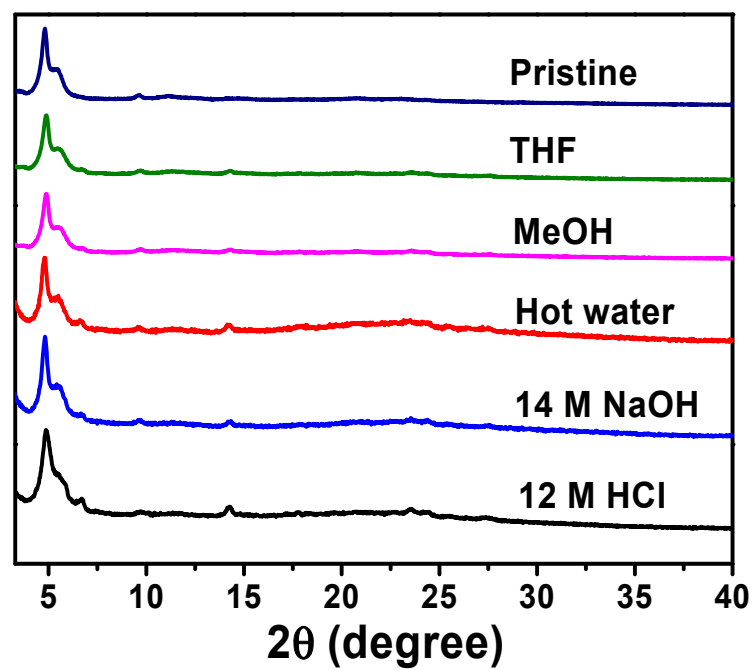**Figure S8.** TGA curve of Co(Ⅱ)@TA-TF COF under N₂.

Figure S9. PXRD patterns of Co(II)@TA-TF COF after treatment for one week at different conditions.
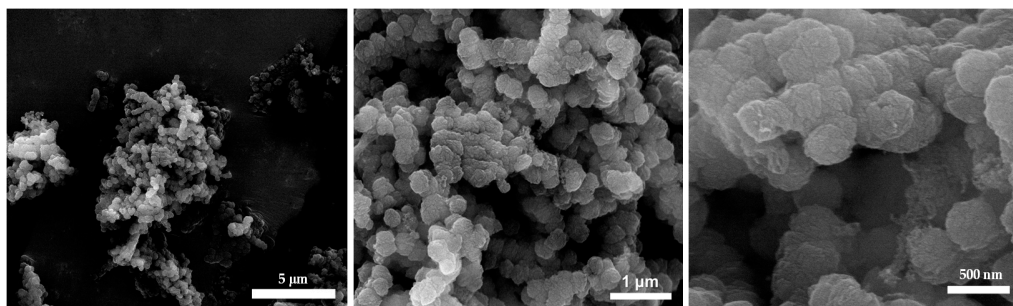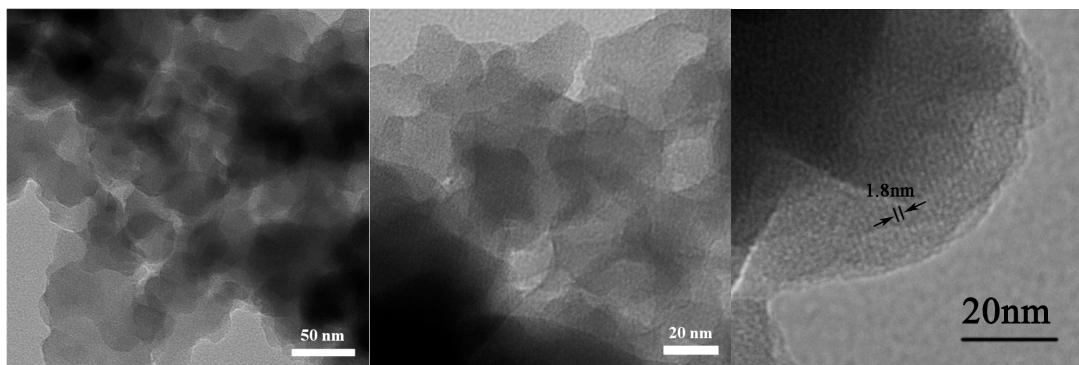

Figure S10. SEM images of Co(II)@TA-TF COF.
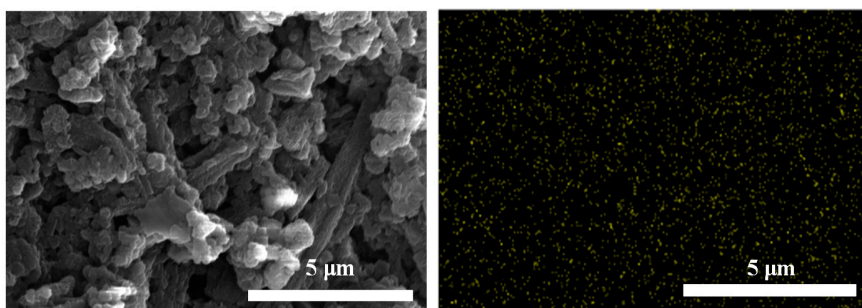
**Figure S11.** TEM images of Co(II)@TA-TF COF.

Figure S12. EDS mapping of Co(II)@TA-TF COF for Co distribution.

Table S3. Comparison of CO_2 uptake ability of various COFs at 298 K.

COFs	S_{BET} (m^2 g^{-1})	CO_2 uptake (wt%)	Reference
Co(II)@TA-TF COF	1076	16.9	herein
COF-5	1670	5.9	S3
TD COF-5	2497	9.2	S4
COF-103	3530	7.6	S3
IL COF-1	2723	6.0	S5
TpPa-1	535	15.6	S6
ACOF-1	1176	17.7	S7
[HO$_2$C]100%-H$_2$PCOF	1176	18	S8

Table S4. Comparison of catalytic performance of Co(II)@TA-TF COF with previously reported COFs and MOFs.

Entry	Catalyst	Substrate	Pressure (MPa)	Temperature (K)	Time (h)	Solvent	Yield (%)		Ref
1	Co(II)@TA-TF COF		0.1	313	48	free	92		**this work**
			0.5	313	48	free	99		**this work**
2	OMe-OH-TPBP-COF		0.1	313	24	/	91		S1
3	CTF-0-400/600-20/20-5		0.69	403	4	free	Conv 100	Select 92.6	S2
4	CCTF-350		0.1	393	24	/	Conv 95	Select 98	S3
5	ImIP@TT-COF		0.1	393	10	free	>99		S4
6	CTF-1-HSA		0.69	403	4	free	Conv 95	Select 98	S5
7	COF 1/ZnBr$_2$		0.1	353	12	free	Conv >99	Select 100	S6
8	COF-PI-2		0.1	324	24	free	99		S7
9	Cu$_x$O$_y$@COF		0.1	308-313	12	free	98		S8
10	COF-JLU7		0.1	313	48	free	92		S9
11	AMIMBr@H$_2$P-DHPh COF		1	393	24	free	91		S10
12	PPS⊂COF-TpBpy-Cu		0.1	313	24	free	95		S11
13	Zn/TPA-TCIF(BD)		0.5	313	10	/	Conv 98.8	Select 99.4	S12
14	CTF-CSU19		0.1	298	48	free	96		S13
15	Co-PCCTF$_5$		0.1	393	24	free	94		S14

No.	Catalyst	Substrate				Solvent	Conv	Select	Ref.
16	COF-salen-Co	Cl-epoxide	2	373	3	/	97	99	S15
17	Zn-CIF2-C$_2$H$_4$	Cl-epoxide	2.5	393	4	/	98	>99	S16
18	COF-TpPa-Py-Br⁻	Cl-epoxide	0.1	373	18	/	>99		S17
19	COF-HNU3	Cl-epoxide	2	373	36	free	96		S18
20	COF-IL	Cl-epoxide	0.1	353	48	free	98		S19
21	ZIF-90-IL-1	Cl-epoxide	2.5	363	8	free	99.12	97.5	S20
22	POM@ImTD-COF	Cl-epoxide	0.1	353	24	free	>99	>99	S21
23	2,5-DCP-CTF	Cl-epoxide	0.69	403	4	free	95		S22
24	CTF-500	Cl-epoxide	1	363	12	/	95		S23
25	NHC-CTFs	Cl-epoxide	0.5	373	6	/	97		S24
26	Co(II)@TA-TF COF	epoxide	0.1	313	48	free	99		**this work**
27	OMe-OH-TPBP-COF	epoxide	0.1	313	24	/	90		S1
28	ImIP@TT-COF	epoxide	0.1	393	24	free	98		S4
29	CTF-P-HSA	epoxide	0.69	403	4	free	83.4	78	S5
30	Cu$_x$O$_y$@COF	epoxide	0.1	308-313	12	free	92		S8
31	IL-ZIF-90	epoxide	1	393	3	free	95		S25
32	AMIMBr@H$_2$P-DHPh COF	epoxide	1	393	24	free	95		S10
33	COF-366-Co(1)/PTAT	epoxide	1.5	393	4	acetonitrile	97.5		S26

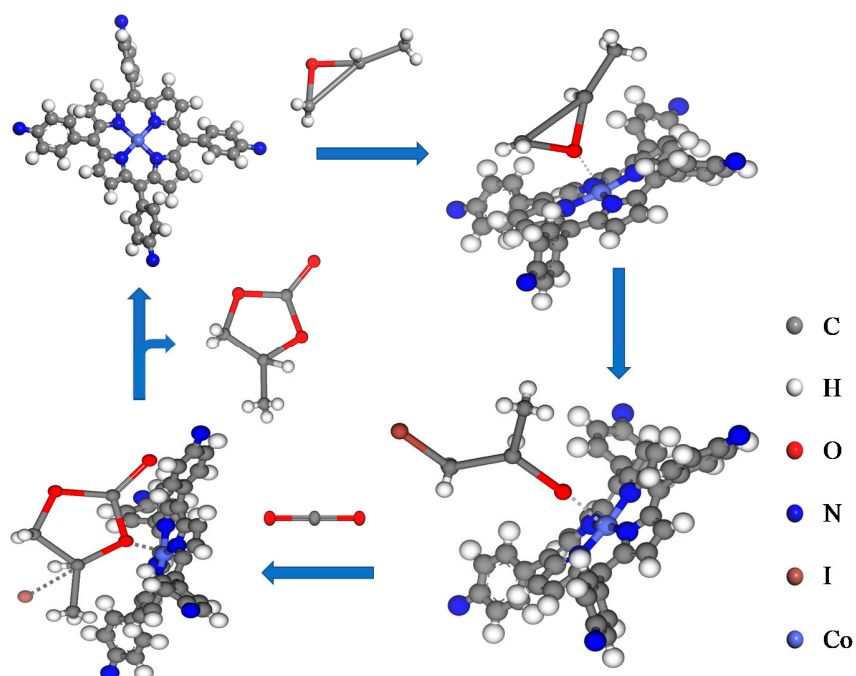|								
34	PPS⊂COF-TpBpy-Cu	0.1	298	72	free	94		S11
35	Zn/TPA-TCIF(BD)	0.5	313	10	/	Conv 99.3	Select 99.7	S12
36	CTF-CSU19	0.1	298	48	free	99		S13
37	COF-salen-Co	2	373	3	/	Conv 91	Select 99	S15
38	COF-HNU3	2	373	48	free	99		S18
39	ZIF-90-IL-1	2.5	363	8	free	Conv 96.27	Select 98.17	S20
40	TpPa-1	0.1	298	8	acetonitrile	86		S27
41	ZIF-90	1.2	393	8	free	81		S28
42	CTF-500	1	363	12	/	99		S23

Figure S13. Scheme of possible catalytic mechanism for the reaction of epoxide and CO_2 into cyclic carbonate catalyzed by Co(II)@TA-TF COF.

Based on the previous reports, a tentative mechanism is proposed for the cycloaddition of epoxide and CO_2 into cyclic carbonate catalyzed by the Lewis acid-based catalyst of Co(II)@TA-TF COF. The COF gave a high catalytic activity on CO_2 conversion because of its exposed metal Co sites located within the centre of porphyrin units, as illustrated in Figure S13. The reaction is initiated by binding the O atom of epoxide (we take propylene oxide as an example here) with the unsaturated Co site in the COF, through which the C-O bond of epoxide is weakened. Subsequently, the I^- generated from tylammonium iodine (TBAI) attacks the less-hindered carbon atom of the coordinated epoxide to open the epoxy ring. After that, CO_2 interacts with the oxygen anion of the opened epoxy ring to form an alkylcarbonate anion, followed by a ring closure step to give the production of cyclic carbonate.
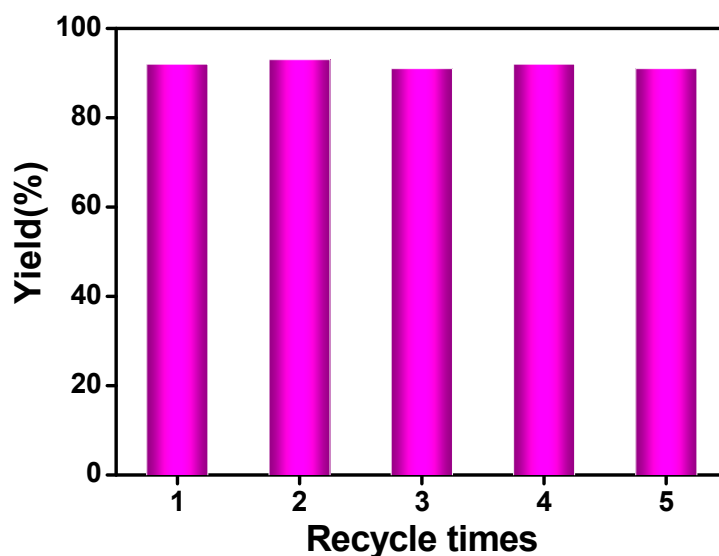

Figure S14. Recyclability test of the Co(II)@TA-TF COF as catalyst for the cycloaddition reaction.
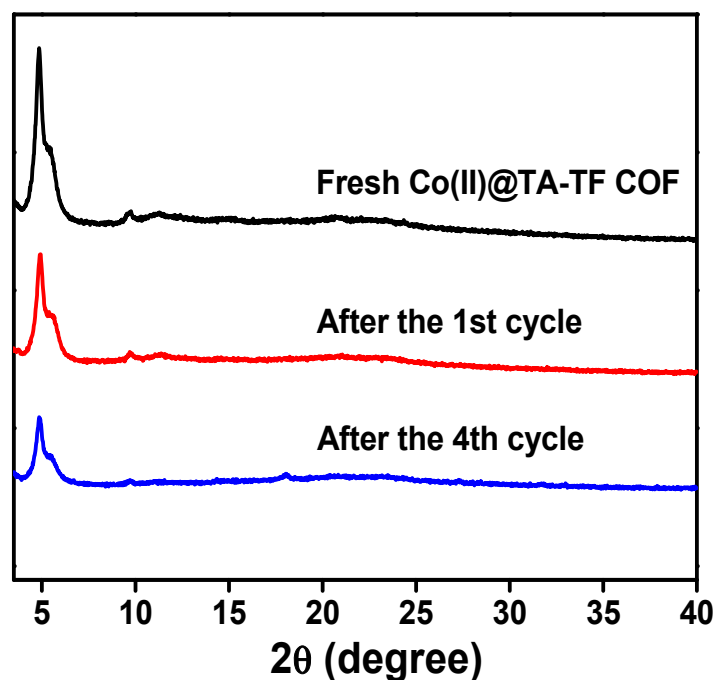
Figure S15. PXRD patterns of the Co(II)@TA-TF COF before and after the recycling test. Epichlorohydrin was selected as a model substrate for this reaction, and all of the other experimental parameters were identical to those presented in Table 1 in the body text.

References

S1. Yang, F.; Li, Y.; Zhang, T.; Zhao, Z.; Chen, L, *Chem. Eur. J.* **2020**, *26*, 4510.

S2. Katekomol, P.; Roeser, J.; Bojdys, M.; Weber, J.; A, Thomas. *Chem. Mater.* **2013**, *25*, 1542.

S3. Liu, T.T.; Xu, R.; Yi, J.D.; Liang, J.; Wang, X.S.; Shi, P.C. *ChemCatChem* **2018**, *10*, 2036.

S4. Zhong, H.; Gao, J.; Sa, R.; Yang, S.; Wu, Z.; Wang, R. *ChemSusChem* **2020**, *13*, 6050-6050.

S5. Jérme R.; Kailasam, K.; Thomas, A.*ChemSusChem* **2012**, *5*, 1793.

S6. Dhankhar, S.S.; Nagaraja, C.M. *Micropor. Mesopor. Mater.* **2020**, *308*, 110314.

S7. Ding, L.; Yao, B.; Wu, W.; Yu, Z.; Wang, X.; Kan, J.; Dong, Y. *Inorg. Chem.* **2021**, *60*, 12591.

S8. Sengupta, M.; Bag, A.; Bordoloi, A.; Islam, M. *J. CO_2 Util.* **2019**, *34*, 533.

S9. Zhi, Y.; Shao, P. Feng, X.; Xia, H.; Zhang, Y.; Shi, Z.; Mu, Y.; Liu, X. *J. Mater. Chem. A* **2018**, *6*, 374.

S10. Zhang, Y.; Hu, H.; Ju, J.; Yan, Q.; Arumugam, V.; J, X.; Cai, H.; Gao, Y. *Chin. J. Catal.* **2020**, *41*, 485.

S11. Sun, Q.; Aguila, B.; Perman, J.; Nguyen, N.; Ma, S. *J. Am. Chem. Soc.* **2016**, *138*, 15790.

S12. Puthiaraj, P.; Kim, H.S.; Yu, K.; Ahn, W.S. *Micropor. Mesopor. Mater.* **2020**, *297*, 110011.

S13. Yu, W.; Gu, S.; Fu, Y.; Xiong, S.; Pan, C.; Liu, Y.; Yu, G. *J. Catal.* **2018**, *362*, 1.

S14. Wu, Q.J.; Mao, M.J.; Chen, J.X.; Huang, Y.B.; Cao, R. *Catal. Sci. Technol.* **2020***, 10,* 8026.

S15. Li, H.; Feng, X.; Shao, P.; Chen, J.; Li, C.; Jayakumar, S.; Yang, Q. *J. Mater. Chem. A* **2019**, *7*, 5482.

S16. Liu, J.; Zhao, G.; Cheung, O.; Jia, L.; Sun, Z.; Zhang, S. *Chem. Eur. J.* **2019**, *25*, 9052.

S17. He, H.; Zhu, Q.Q.; Zhang, W.W.; Zhang, H.W.; Chen, J.; Li, C.P.; Du, M. *ChemCatChem* **2020**, *12*, 5192.

S18. Qiu, J.; Zhao, Y.; Li, Z.; Wang, H.; Shi, Y.; Wang, J. *ChemSusChem* **2019**, *12*, 2421.

S19. Ding, L.G.; Yao, B.J.; Fei, L.; Shi, S.C.; Dong, Y.B. *J. Mater. Chem. A* **2019**, *7*, 4689.

S20. Yuan, H.; Wu, Y.; Pan, X.; Gao, L.; Xiao, G. *Catal. Lett.* **2020**, *150*, 3561.

S21. Zhang Y.; Yang, D.H.; Qiao, S.; Han, B.H. *Langmuir* **2021**, *37*, 10330.

S22. Li, Y.M.; Yang, L.; Sun, L.; Ma, L.; Li, Z. *J. Mater. Chem. A* **2019**, *7*, 26071.

S23. Buyukcakir, O.; Sang, H.J.; Talapaneni, S.N.; Kim, D.; Coskun, A. *ACS Appl. Mater. Interfaces* **2017**, *9*, 7209.

S24. Yue, C.; Wang, W.; Li, F. *ChemSusChem* **2020**, *13*, 5996.

S25. Tharun, J.; Bhin, K.M.; Roshan, R.; Kim, D.W.; Kathalikkattil, A.C.; Babu, R.; Ahn, H.Y.; Wonc, Y.S.; Park, D.W. *Green Chem.* **2016**, *18*, 2479.

S26. Xu, K.; Dai, Y.; Ye, B.; Wang, H. *Dalton Trans.* **2017**, *46*, 10780.

S27. Das, A.; Mondal, R.K.; Chakrabortty, P.; Riyajuddin, S.; Chowdhury, A.H.; Ghosh, S.; Khan, A.; Ghosh, K.; Islam, S.M. *Mol. Catal.* **2021**, *499*, 111253.

S28. Tharun, J.; Mathai, G.; Kathalikkattil, A.C.; Roshan, R.; Won, Y.S.; Cho, S.J.; Chang, J.S.; Park, D.W. *ChemPlusChem* **2015**, *80*, 715.